An electrostatic interaction between TEA and an introduced pore aromatic drives spring-in-the-door inactivation in *Shaker* potassium channels

Christopher A. Ahern,[1,2] Amy L. Eastwood,[3] Dennis A. Dougherty,[3] and Richard Horn[4]

[1]Department of Anesthesiology, Pharmacology and Therapeutics, and [2]Department of Cellular and Physiological Sciences, The University of British Columbia, Vancouver, British Columbia V6T 1Z3, Canada
[3]Division of Chemistry and Chemical Engineering, California Institute of Technology, Pasadena, CA 91125
[4]Department of Molecular Physiology and Biophysics, Institute of Hyperexcitability, Jefferson Medical College, Philadelphia, PA 19107

Slow inactivation of Kv1 channels involves conformational changes near the selectivity filter. We examine such changes in *Shaker* channels lacking fast inactivation by considering the consequences of mutating two residues, T449 just external to the selectivity filter and V438 in the pore helix near the bottom of the selectivity filter. Single mutant T449F channels with the native V438 inactivate very slowly, and the canonical foot-in-the-door effect of extracellular tetraethylammonium (TEA) is not only absent, but the time course of slow inactivation is accelerated by TEA. The V438A mutation dramatically speeds inactivation in T449F channels, and TEA slows inactivation exactly as predicted by the foot-in-the-door model. We propose that TEA has this effect on V438A/T449F channels because the V438A mutation produces allosteric consequences within the selectivity filter and may reorient the aromatic ring at position 449. We investigated the possibility that the blocker promotes the collapse of the outer vestibule (spring-in-the-door) in single mutant T449F channels by an electrostatic attraction between a cationic TEA and the quadrupole moments of the four aromatic rings. To test this idea, we used in vivo nonsense suppression to serially fluorinate the introduced aromatic ring at the 449 position, a manipulation that withdraws electrons from the aromatic face with little effect on the shape, net charge, or hydrophobicity of the aromatic ring. Progressive fluorination causes monotonically enhanced rates of inactivation. In further agreement with our working hypothesis, increasing fluorination of the aromatic gradually transforms the TEA effect from spring-in-the-door to foot-in-the-door. We further substantiate our electrostatic hypothesis by quantum mechanical calculations.

INTRODUCTION

Voltage-gated potassium channels play a critical role in shaping electrical signals in the cardiovascular and nervous systems. For many of these channels, depolarization of the plasma membrane produces a rapid activation of potassium current, followed by a typically slower loss of conductance known as inactivation. The rate and extent of inactivation are regulated in a variety of ways to fine-tune the contribution of these membrane proteins to a cell's excitability. One mechanism, termed "slow inactivation," predominates under conditions of prolonged depolarization that either occur naturally or are associated with arrhythmogenic or epileptic conditions. Experimental, computational, and structural investigations into the mechanism of slow inactivation, labeled C-type inactivation in several types of potassium channels (Hoshi et al., 1991), suggest that rearrangements at the selectivity filter and extracellular entrance to the pore result in a constricted, nonconducting permeation pathway (López-Barneo et al., 1993; Yellen et al., 1994;

Yellen, 1998, 2002; Cordero-Morales et al., 2006a,b, 2007; Chakrapani et al., 2007a,b).

Quaternary ammonium compounds have long been used to investigate the mechanistic details of gating and selectivity in ion channels. One example relevant to the present experiments, the external application of the pore blocker TEA, has been shown to inhibit slow inactivation in wild-type *Shaker* potassium channels (Liu et al., 1996). This phenomenon, termed foot-in-the-door (Yeh and Armstrong, 1978), has been rationalized as being due to obstruction of the constriction of the external vestibule when the blocker is bound there. Subsequent structural analysis of the prokaryotic *Shaker* homologue KcsA, solved in the presence of the TEA analogue tetraethylarsonium, places the blocker at a site near the extracellular entrance to the permeation pathway where it could interfere with pore collapse (Lenaeus et al., 2005). Experimental use of TEA has also been helpful in distinguishing the different types of potassium channel

Correspondence to Christopher A. Ahern: cahern@interchange.ubc.ca

isoforms because only those that possess an aromatic phenylalanine or tyrosine at the position equivalent to 449 in *Shaker* at the extracellular entrance to the permeation pathway bind extracellular TEA with high affinity (MacKinnon and Yellen, 1990; Kavanaugh et al., 1991; Molina et al., 1997). We have shown previously that in *Shaker* channels, this aromatic prerequisite is due largely to a cation–π interaction between the cationic blocker and the negative electrostatic potential on the face of the aromatic side chain (Ahern et al., 2006). This conclusion was established experimentally with unnatural amino acid mutagenesis and computationally with ab initio calculations based on an existing potassium channel structure. These results have structural implications because this type of electrostatic interaction, unlike a salt bridge, is strongly constrained geometrically and is supported only when the cation interacts with the face, not the edge, of the side chain's aromatic ring. We call this orientation of the aromatic ring "en face" with respect to the fourfold symmetry axis of the channel. This is noteworthy because in high-resolution structures of the prokaryotic channel KcsA, the side chain of the aligned residue (Y82) is usually oriented "edge-on," meaning that the edge of the aromatic ring faces the central axis of the pore (Doyle et al., 1998). This raises the possibility that although similar, the details of the selectivity filter architecture could differ between *Shaker* and KcsA, and these differences could contribute to the mechanisms of channel inhibition.

The experiments described here show that external application of TEA accelerates slow inactivation in the T449F *Shaker* channels. This accelerating effect is well described by a simple mechanism in which slow inactivation involves collapse of the external entrance of the permeation pathway. We propose that TEA binding encourages collapse due to the attraction between the negative electrostatic potential on the face of the aromatic side chain at position 449 and the cationic blocker in the central axis of the permeation pathway. We test this possibility directly by expressing serially fluorinated derivatives of phenylalanine at the 449 position and investigating the effects of this manipulation on slow inactivation in the presence and absence of TEA. In *Shaker* channels carrying a second mutation in the pore helix, V438A, the effect of external TEA reverts to the traditional foot-in-the-door inhibition of slow inactivation. We posit that the V438A mutation, in a manner reminiscent of the homologous E71A mutation in KcsA (Cordero-Morales et al., 2006b) causes the aromatic side chain at 449 to reorient in relation to the permeation pathway, and in doing so abolishes the cation–π attraction between blocker and the aromatic side chain. Lastly, we use ab initio quantum mechanical calculations to test a simplified interaction model between the four *Shaker* aromatic side chains and TEA. The calculations are consistent with a model in which TEA binding energetically

favors the collapse of the external vestibule, in support of our experimental conclusions. These observations, in combination with previous results, serve to further refine our understanding of the mechanistic rearrangements that cause slow inactivation in *Shaker* channels.

MATERIALS AND METHODS

Molecular biology and unnatural amino acids
The channel we used was *Shaker* H4 with the following three modifications: deletion of residues 6–46 to remove N-type inactivation and the point mutations C301S and C308S. The in vivo nonsense suppression methodology was performed as described previously (Nowak et al., 1995, 1998). The 449 and 438 sites of *Shaker* cDNA were mutated by conventional mutagenesis (Agilent Technologies), and complementary mRNA was transcribed from this cDNA (mMessage mMachine; Applied Biosystems). Unnatural amino acids (aa) were protected with nitroveratryloxycarbonyl, activated as the cyanomethyl ester, and coupled to the dinucleotide dCA. This aminoacyl dinucleotide was then ligated to a modified tRNA from *Tetrahymena thermophila*. Deprotection of the aminoacylated tRNA-aa was performed by UV irradiation immediately before coinjection with the cRNA for the channel into stage V–VI *Xenopus* oocytes. Typically, 20 ng tRNA-aa and 25 ng cRNA were injected in a 50-nl volume.

Electrophysiology
Voltage-clamped potassium currents were recorded with two microelectrodes using a voltage clamp (OC-725C; Warner) in a standard Ringers solution (in mM): 116 NaCl, 2 KCl, 1 MgCl$_2$, 0.5 CaCl$_2$, and 5 HEPES, pH 7.5.

Computations
For ab initio calculations, we used Jaguar software (version 7.0; Schrödinger). The molecular models and their coordinates are described in the Discussion. We determined the single-point gas-phase energies of these structures using a pseudo-spectral implementation of localized Møller-Plesset perturbation theory (LMP2) (Saebo and Pulay, 1993; Murphy et al., 1995) with Boys-localized valence orbitals (Foster and Boys, 1960) and the 6-31G* basis set. For each structure, the change in free energy during collapse was calculated in the presence (ΔE_{TEA}) and absence (ΔE_{empty}) of TEA. The effect of TEA on the collapse is defined as $\Delta\Delta E = \Delta E_{TEA} - \Delta E_{empty}$. For estimates of electrostatic potential in water, we used a self-consistent reaction field method with the Poisson-Boltzmann solver in Jaguar, using the 6–31+G* basis set.

RESULTS

We demonstrated previously that the extracellular TEA blockade of *Shaker* T449F channels relies heavily on an electrostatic, cation–π interaction between the blocker and the aromatic side chain at this site. These results could be fully explained with a *Shaker* blocking model based on atomic resolution structures of KcsA where four aromatic side chains simultaneously present their negative electrostatic potential focused on their faces toward the blocker. One prediction of this model is that under a prolonged depolarizing stimulus, TEA could actually facilitate pore collapse through attractive forces between the blocker and the four aromatic side chains. This

prediction runs counter to the canonical foot-in-the-door inhibition of slow inactivation characterized previously in wild-type *Shaker* channels. We therefore aimed to refine our mechanistic understanding of slow inactivation by investigating the interaction between TEA and an introduced phenylalanine residue at position 449. A previous study showed that an aromatic substitution at this position (T449Y) reduced the rate of slow inactivation by ~30-fold (Molina et al., 1997). We assume that the mechanism of slow inactivation is fundamentally the same in the T449F mutant as in a wild-type channel, a conclusion also supported by studies of KcsA that has a tyrosine (Y82) at the aligned residue of *Shaker*'s T449 (Cordero-Morales et al., 2006b). Another possibility, that the T449F mutation abolishes C-type inactivation, revealing a U-type inactivation (Klemic et al., 2001), will be addressed in the Discussion.

The residue Y82 of KcsA is displayed in Fig. 1 A to illustrate the relationship between the aromatic side chain and the permeation pathway. Fig. 1 B shows the effect of increasing concentrations of externally applied TEA on slow inactivation of T449F *Shaker* channels during a 50-s depolarization to +40 mV. The traces, normalized to the peak value to allow for the comparison of the inactivation rates, are accurately fit by a single-exponential relaxation. We designate the accelerating effect of TEA block as "spring-in-the-door," a phenomenon opposite to the canonical foot-in-the-door process demonstrated previously with wild-type *Shaker* channels carrying a non-aromatic residue at the 449 site. Similar to the previous analyses of external TEA blockade, the present results are described with a three-state model (Fig. 1 C), except that T449F channels inactivate more rapidly from the blocked than from the open state.

A previous structural study of KcsA has shown that the E71A mutation in the pore helix of KcsA may serve to reorient Y82 from edge on to en face in structural studies, while effectively abolishing inactivation (Cordero-Morales et al., 2006b). The inset in Fig. 2 A shows the structure of KcsA (PDB, 1ZW1), demonstrating the physical proximity of the pore aromatic Tyr82 and E71A (highlighted by arrow). We tested whether alanine substitution of the homologous *Shaker* residue, V438, could similarly inhibit inactivation and, more importantly, how this might impact external blockade by TEA. Fig. 2 A shows a family of potassium currents in response to depolarizing steps between −40 and +60 mV from a holding potential of −100 mV. The double mutation V438A/T449F accelerates the rate of slow inactivation ~50-fold at +40 mV, compared with the single mutant T449F. Inhibition by TEA for the two channel types is shown in Fig. 2 B. The V438A mutation reduces the affinity of the channel for TEA approximately fivefold from 0.4 ± 0.04 to 1.9 ± 0.2 mM for T449F and V438A/T449F channels, respectively. For comparison, the K_i for external TEA binding to wild-type KcsA, a channel with an edge-on
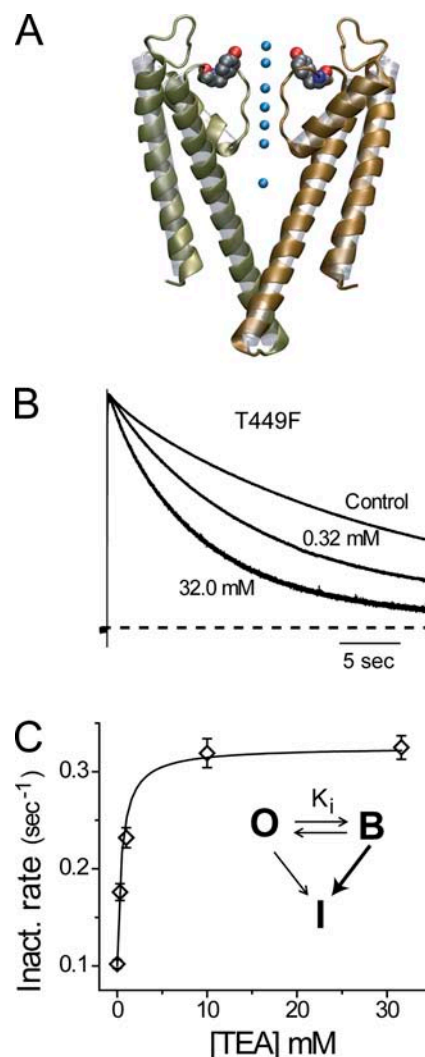

Figure 1. Extracellular TEA accelerates slow inactivation in T449F *Shaker* channels. (A) KcsA crystal structure with Y82 shown in space filling representation; PDB, 1K4C. (B) Outward potassium currents in response to a 50-s depolarizing pulse to +40 mV from a holding potential of −100 mV for control and in the presence of the indicated TEA concentration. Traces are normalized to their peak current value to facilitate comparison of the inactivation kinetics. As opposed to the traditional slowing behavior of TEA on inactivation, here the accelerating effect motivates the terminology "spring-in-the-door." (C) The rate of inactivation is the inverse of the time constant for a single-exponential fit to the relaxation and is well fit by a three-state model (inset) in which inactivation is more rapid from the blocked state. Let k_{OI} be the inactivation rate constant from the open state (O) to the inactivated state (I), and k_{BI} the inactivation rate constant from the blocked state (B). The equilibrium probability of fast block in the absence of inactivation is $P_{block} = (1 + K_i / [TEA])^{-1}$. The observed inactivation rate is then defined as $\rho = k_{BI}P_{block} + k_{OI}(1 - P_{block})$. Values of k_{OI} and P_{block} were estimated separately, leaving only k_{BI} to be estimated from the data in C. We propose that electrostatic attraction contributes to TEA collapse in the single mutant due to the en face orientation of the aromatic rings.

orientation of the equivalent pore aromatic Y82, is ~3 mM (Heginbotham et al., 1999). Fig. 2 C shows the effect of external TEA on the rate of inactivation at
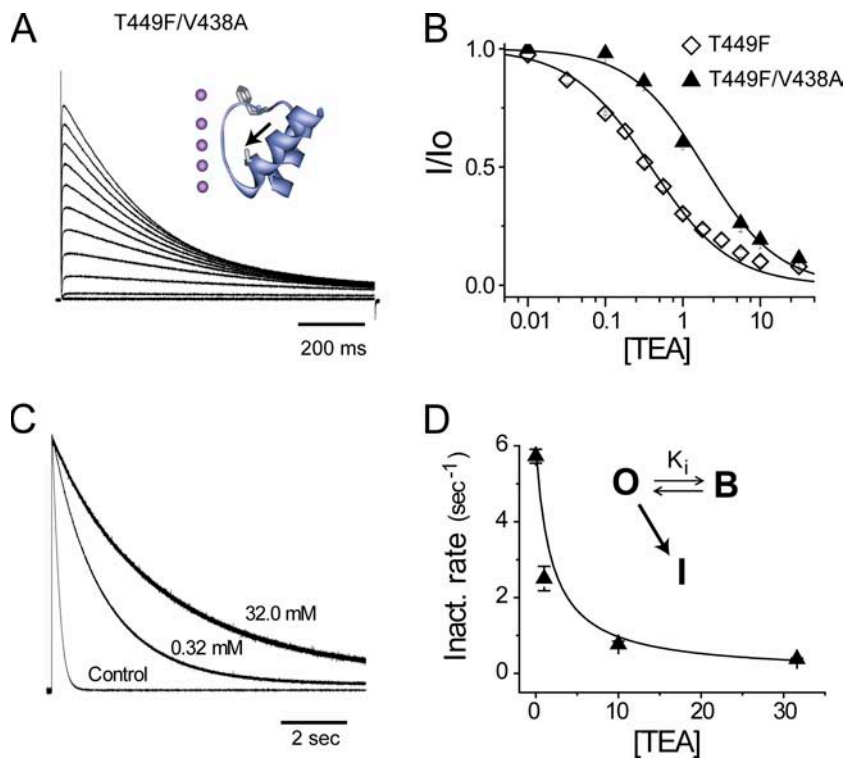
Figure 2. The V438A mutation enhances slow inactivation, lowers TEA affinity, and restores foot-in-the-door blockade in *Shaker* T449F channels. (A) Potassium currents from the double V438A/T449F mutant in response to 1-s depolarizations from −80 to +100 mV in 20-mV steps. The inset shows the structure of KcsA (PDB, 1ZW1) with the side chains shown for the aromatic Y82 and E71A (highlighted by arrow). The corresponding *Shaker* residues are 449 and 438, respectively. (B) Inhibition of the mutants by extracellular TEA. Smooth lines represent standard binding isotherms with inhibitory constants of 0.39 and 1.97 mM for T449F and V438A/T449F, respectively. (C) Normalized outward potassium currents from V438A/T449F channels in increasing TEA concentrations. The V438A mutation speeds slow inactivation from τ_{inact} = 9.9 ± 0.4 s to τ_{inact} = 0.18 ± .01 s at +40 mV for T449F (n = 14) and V438A/T449F (n = 5) channels, respectively, with the number of cells in parentheses. (D) The speeding can also be explained by a three-state model in which inactivation only occurs from the open state. The smooth line through the data points is a theory curve generated from known values. See equations in the legend of Fig. 1, with k_{BI} = 0.

+40 mV for normalized potassium currents from V438A/T449F channels. In each case, the current decay was fit by a single-exponential relaxation with the corresponding rates ($1/\tau_{inact}$) plotted in Fig. 2 D, demonstrating that the V438A mutation serves to restore the canonical foot-in-the-door effect on slow inactivation. The solid curve through the data points was not a statistical fit; rather, it was generated with known values (K_i, [TEA] and τ_{inact} in the absence of TEA) in accordance with the foot-in-the-door model (see legend to Fig. 2 C). A possible explanation for this effect is that in *Shaker*, as in KcsA, the V438A mutation reorients the aromatic side chain at position 449. For example, although the aromatic ring in the single mutant T449F has an en face orientation (Ahern et al., 2006), it might have an edge-on orientation in the double mutant V438A/T449F. If this were indeed the case, in the double mutant TEA would interact with the positive electrostatic potential concentrated toward the edge of the aromatic ring, causing an electrostatic repulsion between the blocker and the side chain, a scenario that could reasonably obviate pore collapse.

Serial fluorination of aromatic side chains is a powerful tool in the investigation of putative cation–π interactions because this straightforward modification isolates the electrostatic component of the interaction energy while leaving the polarizability, hydrophobicity, sterics, and charge of the side chain relatively unperturbed (Ma and Dougherty, 1997). In considering the possible consequences of fluorination in the present system, we begin with two assumptions: the aromatic

rings in the single mutant T449F adopt an en face orientation (Ahern et al., 2006), and inactivation brings the aromatic side chains closer to the central axis of the permeation pathway. When no TEA is present, the faces of the four aromatic rings point toward each other, and although they are significantly separated in space, they should experience a weak repulsion due to the negative electrostatic potentials. Based on this hypothetical structural model, we predict two consequences of fluorinating the aromatic ring at position 449 in a channel containing the native residue Val438. First, serial fluorination will monotonically increase the rate of inactivation because this manipulation reduces the aforementioned negative electrostatic potential, allowing the aromatics to approach the central axis with less energetic penalty. The second prediction, also based on electrostatic considerations, is that the spring-in-the-door effect of TEA (Fig. 1, B and C) will be monotonically ameliorated by serial fluorination, which reduces the attraction between TEA and the 449 aromatic (Ahern et al., 2006).

The first prediction is confirmed because serial fluorination enhances the rate of inactivation, as shown by the normalized currents in Fig. 3 A. This observation is quantified in Fig. 3 B, where the time to 50% inactivation is plotted for each channel type. Although the inactivation kinetics are complex and the overall effect is not large, the clearly accelerating trend for each added fluorine makes a strong case for the model.

The second prediction, that fluorination of this aromatic will reduce the spring-in-the-door effect of TEA,
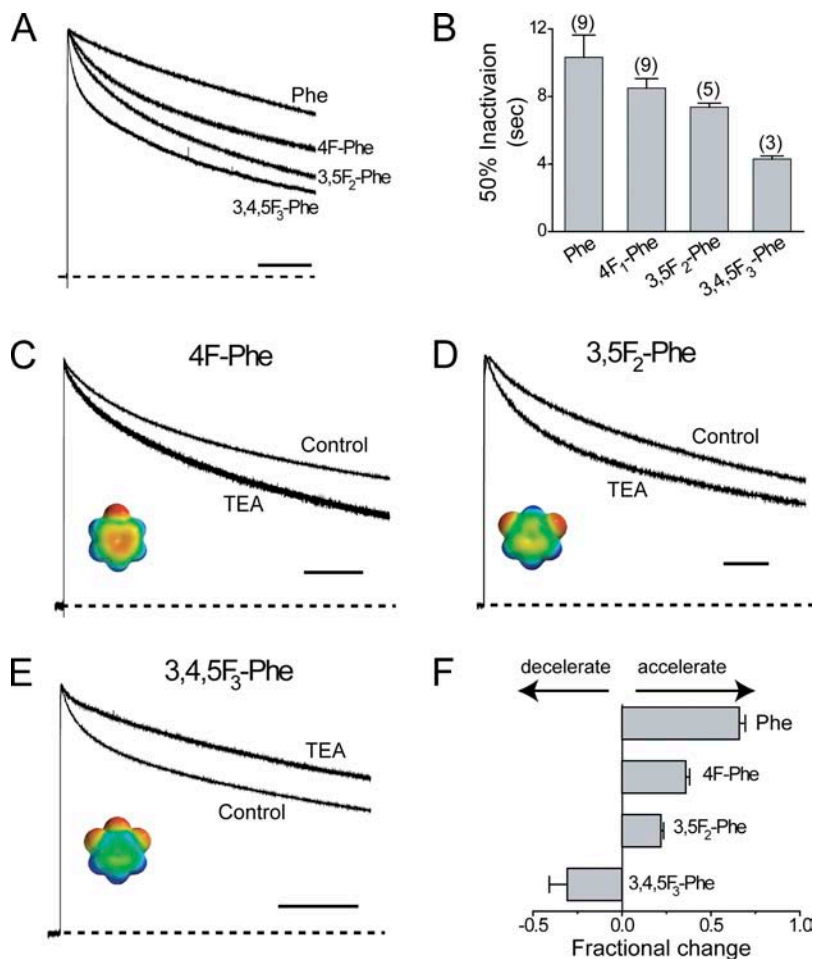
Figure 3. Serial fluorination of phenylalanine at position 449 reveals a role for a cation–π interaction in the TEA effects on slow inactivation. (A) Normalized representative currents in response to a 10-s depolarization to +40 mV from a holding potential of −100 mV for *Shaker* channels with the indicated side chain at the 449 position. (B) Time to 50% inactivation for the indicated channel types (number of cells in parentheses) shows a gradual and stepwise accelerating trend in the slow inactivation with each added fluorine. (C–E) Representative currents for the indicated phenylalanine derivative at the 449 position with and without TEA. Each channel type was temporally "normalized" where the control recording reached 50% inactivation at the end of the pulse. Scale bars represent 1 s for each channel type. TEA concentrations used (in mM): 10 (3.3), 56 (48), and 116 (175) for 4F$_1$-Phe, 3,5F$_2$-Phe, and 3,4,5F$_3$-Phe, respectively, with the measured K_i for the channel type in parentheses. (F) Fractional change in the effect of TEA on the amount of current at 50% inactivation for the indicated channel types (number of cells in parentheses). We suggest the inversion of behavior from spring-in-the-door to foot-in-the-door is due to the reduction of negative electrostatic potential on the face of the four aromatic residues due to serial fluorination.

was also validated experimentally. Fig. 3 (C–E) shows representative current traces for the indicated channel types, demonstrating the effect of fluorination on slow inactivation of TEA-blocked channels. The inset images illustrate the effect of fluorination on the aromatic for each channel type, with red and blue as negative and positive electrostatic potential, respectively. These data show that increasing fluorination converts the effect of TEA from spring-in-the-door to foot-in-the-door (Fig. 3, C–F). Interestingly, the switch from TEA accelerating to decelerating the rate of inactivation occurs when the difluorinated derivative receives a third fluorine (Fig. 3, D and E). Notably, tri-fluorination causes the electrostatic potential of the aromatic face to reverse sign from strongly negative to slightly positive (Santarelli et al., 2007). Therefore, TEA block of the channel with a tri-fluorinated aromatic at the 449 site is expected to inhibit collapse for electrostatic reasons, as we observe. We quantified this phenomenon by comparing the time to the 50% inactivation level for control and TEA-blocked channels (Fig. 3 F). We suggest that the systematic reduction by fluorine of negative electrostatic potential on the face of the aromatic ring results in a stepwise loss of attraction between the side chain and the blocker. This

in turn first reduces, then reverses, the pore collapse promoted by TEA's interaction with the aromatic side chain, as the electrostatic forces change from attractive to repulsive.

DISCUSSION

The conformational transformation that produces slow inactivation is not known. However, several lines of evidence, both experimental and theoretical, suggest that slow inactivation is accompanied by movement in the vicinity of the extracellular region of the permeation pathway, including the selectivity filter. In most proposals, the closing of the slow inactivation gate involves a constriction of the pore, creating an unsurpassable energy barrier for the transit of K$^+$ ions (Liu et al., 1996; Starkus et al., 1997; Kiss et al., 1999; Bernèche and Roux, 2005; Cordero-Morales et al., 2007; Ader et al., 2008). However, conformational movements external to and on the backside of the selectivity filter (within the pore helix) have also been proposed. The magnitude of these conformational changes has not been resolved, in part because an unambiguous structure of the inactivated state is not yet available. Nevertheless,

slow inactivation might produce movements as large as several angstroms for both side chains and the protein backbone near the selectivity filter (Bernèche and Roux, 2005; Cordero-Morales et al., 2006b, 2007; Stansfeld et al., 2008).

Permeant ions and extracellular pore blockers have profound effects on slow inactivation in *Shaker* and related Kv channels. In general, for these channels, the binding of permeant ions inhibits slow inactivation, essentially stabilizing an open/conducting conformation (López-Barneo et al., 1993; Baukrowitz and Yellen, 1995), and small cationic blockers, like extracellular TEA, prevent the inactivation gate from closing (Grissmer and Cahalan, 1989; Choi et al., 1991). However, not all extracellular blockers produce foot-in-the-door inhibition of slow inactivation. For example, charybdotoxin, a 37–amino acid neurotoxin, blocks *Shaker* potassium channels with high affinity, without affecting either activation gating or slow inactivation (Goldstein and Miller, 1993; Liu et al., 1996). Of particular relevance to our study, extracellular TEA had no effect on slow inactivation kinetics for the *Shaker* double mutant D447E/T449Y (Molina et al., 1997). As we show here, the single mutant T449F not only abolishes TEA's canonical foot-in-the-door effect, but it also reverses its sign, inspiring a blocked channel to inactivate more rapidly.

Our previous results suggest that an introduced phenylalanine residue at the 449 site has an en face orientation (Ahern et al., 2006). If we accept this premise, and also that slow inactivation is accompanied by a constriction of the extracellular mouth of the pore, it remains for us to explain the two dramatic consequences of fluorinating these residues on the rate of slow inactivation. First, progressive fluorination of the aromatic speeds inactivation. Second, fluorination converts the effect of TEA block from spring-in-the-door to foot-in-the-door (Fig. 3). We propose that both of these experimental phenomena may be accounted for largely by electrostatics.

First, the en face orientations of the four aromatic residues necessitate a mutual electrostatic repulsion that would tend to inhibit pore collapse, and this repulsion would be decreased by fluorination. Second, the electrostatic attraction between an aromatic residue and the cationic TEA molecule in its binding site would be diminished by fluorination, thus reducing the influence of TEA and slowing the rate of inactivation of a blocked channel.

To investigate the merits of our electrostatic hypothesis in greater detail, we used high-level (gas-phase MP2) ab initio calculations to model edge-on versus en face pore collapse in the presence and absence of TEA. The structural model (Fig. 4 A) is based on the crystal structure of the tetraethylarsonium-blocked KcsA channel (Lenaeus et al., 2005). The blocker was converted to TEA by substituting a nitrogen atom for arsenic, followed by

optimization (Ahern et al., 2006). The only contributions from the channel were the four aromatic rings from the Y82 side chains of KcsA (Fig. 4 A, top left). The en face conformation was created by rotating the aromatic ring 60° along the $C_\beta C_\gamma$ bond of Y82 (Ahern et al., 2006), as shown in the bottom left-hand panel of Fig. 4 A. We simplistically modeled inactivation by a modest 1.5-Å translation of each aromatic ring toward the central axis (Fig. 4 A, right-hand panels). The quantum mechanical energies of these four structures were determined in the presence and absence of TEA. For the edge-on conformation, TEA had only a small effect on collapse energetics (Fig. 4 B), whereas in the en face conformation, TEA clearly favored collapse ($\Delta\Delta E = -4.4$ kcal/mol).
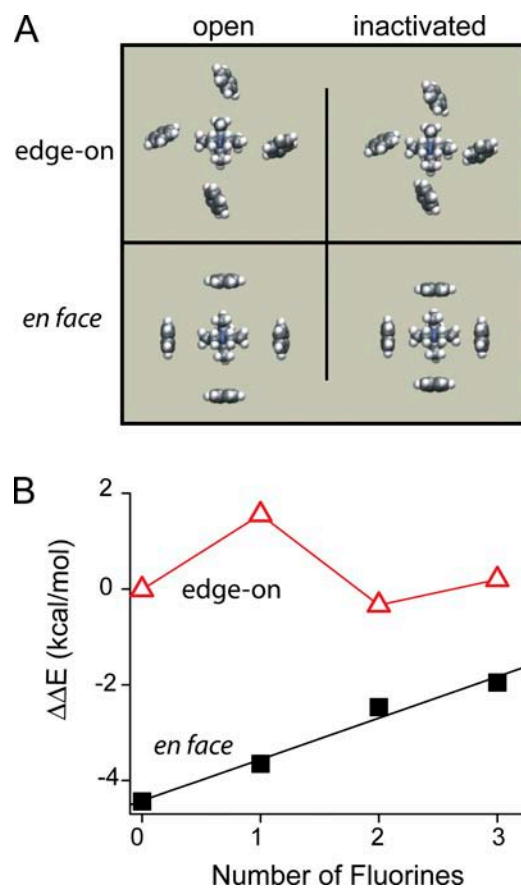

Figure 4. Model of pore collapse with TEA for the en face and edge-on conformations. (A, left) A bird's eye view of two proposed conformations of the aromatic rings of T449F from the edge-on crystal structure of KcsA with TEAs (Lenaeus et al., 2005) and the en face conformation (Cordero-Morales et al., 2006b; Ahern et al., 2006). (Right) A putative "collapse" of this region during slow inactivation, as each aromatic ring was moved 1.5 Å toward the central axis of the pore. (B) The plot shows the effect of fluorinating the aromatic rings on TEA's contribution to the energetics of collapse. The ab initio calculations were done at the MP2 level. Tri-fluorination had little effect (<0.3 kcal/mol) for the edge-on conformation. Consistent with our experimental data, however, increased fluorination causes a monotonically inhibitory effect of TEA on collapse for the en face conformation, where tri-fluorination increases $\Delta\Delta E$ by 2.5 kcal/mol.

Presumably, this difference is largely a consequence of cation–π electrostatics, consistent with our previous calculations (Ahern et al., 2006).

The repulsive electrostatic component in our model can be quantified by calculating the effect of collapse on the electrostatic potential in the radial center of the permeation axis between the four aromatic rings (at site S0; see Materials and methods for details). In the en face orientation, this electrostatic potential increases from −144 to −228 mV upon collapse (Fig. 4 A). This corresponds to a free energy change (ΔΔG) of 1.9 kcal/mol. This is the repulsive electrostatic energy that would inhibit collapse, and it would be smaller in magnitude for fluorinated derivatives. It is also possible that fluorination affects the affinity of a permeant ion at the extracellular entrance (site S0) of the permeation pathway. Fluorination is expected to lower this affinity in the en face conformation, and when S0 is unoccupied, the outer vestibule might collapse more easily. Note that a smaller repulsive electrostatic potential and energy is associated with the collapse of the edge-on conformation (collapse increases the electrostatic potential from +22.9 to +42.4 mV; ΔΔG = 0.45 kcal/mol). The smaller magnitude of the electrostatic potential for the edge-on conformation is due to the fact that the aromatic rings are rotated only 60°, not 90°, from the full en face orientation. We further characterized these models by determining TEA's predicted effect on collapse energetics with the fluorinated derivatives. Fig. 4 B shows that fluorination has only a moderate energetic effect in the edge-on model. The dip in energy for the di-fluorinated benzene rings is exactly what we observed previously for this type of model (Ahern et al., 2006), and it is explained by an electronegative fluorine atom pointing toward the cationic blocker. The data therefore argue against an "induced-fit" model of TEA binding, wherein the fluorine atoms cause the aromatic side chains to twist in promoting an enhanced interaction with the blocker. Furthermore, the nonmonotonic trend of the effects of fluorination for the edge-on model is inconsistent with our experimental data. In contrast, in the en face model, each added fluorine destabilizes the collapse by 0.86 kcal/mol, consistent with our experimental observation that progressive fluorination of phenylalanine at position 449 monotonically weakens TEA's spring-in-the-door effect, gradually converting it to foot-in-the-door. However, the predicted magnitude of the effect of fluorination (∼85-fold change of rate for tri-fluorination) is larger than we observe experimentally. This quantitative discrepancy is undoubtedly due to the simplicity of the model, which is missing many molecular participants in binding and collapse, including water, not to mention the fact that we are awaiting an atomic-level structure of the inactivated state. Nevertheless, this analysis adds further support for the postulated role of electrostatics in slow inactivation for T449F channels, and

for the concept that slow inactivation might be accompanied by a general constriction of the selectivity filter. It is worth noting here that rotations of the aromatic ring along the $C_\beta C_\gamma$ bond are likely to involve conformational changes along the peptide backbone because of the energetic cost of the side chain assuming an unusual rotamer torsion angle (see Cordero-Morales et al., 2006b).

Inactivation involves residues some distance from the outer mouth of the permeation pathway, notably including a residue behind the selectivity filter near the bottom of the pore helix. This residue, E71 in KcsA, when mutated to an alanine, may indeed cause significant alterations of the peptide backbone in the vicinity of the selectivity filter, as seen in the "flipped conformation" reported in Cordero-Morales et al. (2006b). One consequence of the E71A mutation is a rotation of Y82's aromatic rings in KcsA into an en face conformation. The alanine mutation of the residue homologous to KcsA's E71 (V438 in *Shaker*) has three significant effects. The first is a fivefold decrease in TEA affinity, the second is a 50-fold increase in the rate of slow inactivation, and the third is a conversion of spring-in-the-door to foot-in-the-door. All three can be explained simply if the V438A mutation causes the aromatic at 449 to rotate from an en face to an edge-on conformation. For this scenario, the decrease in TEA affinity would be due to the loss of the cation–π contribution to TEA binding that would be concomitant with such a rotation of the side chain. In fact, the resultant inhibition constant of the V438A mutant (∼2.0 mM) is similar in magnitude to that of wild-type KcsA (∼3.0 mM), in which Y82 has an edge-on orientation. The speeding of inactivation is predicted from our quantum mechanical calculations, although the magnitude of the effect observed experimentally is larger than that predicted by the model in Fig. 4. Notably, mutations of the homologous pore helix residue in Kv1.2 also speed inactivation kinetics (Cordero-Morales et al., 2007). Finally, the effect of TEA binding on inactivation is expected to change sign if the aromatic rings rotate from en face to edge-on, as shown above. Although such a dramatic consequence of the V438A mutation on a distant residue might appear implausible, a 60° rotation of the aromatic ring of Y82 is observed in KcsA for the flipped conformation of the E71A mutation, although in the opposite direction, namely from edge-on to en face (Cordero-Morales et al., 2006b). This scenario emphasizes the potential importance of allosteric cross talk between relatively distant regions of the ion channel protein.

We have presented a relatively simplistic model of slow inactivation in which electrostatics plays a significant role. This model is reasonably self-consistent with our experimental and theoretical observations for *Shaker* channels harboring the T449F mutation. However, slow inactivation is likely to be much more complicated than this model, possibly including substantial backbone

alterations in the vicinity of the selectivity filter. For example, our data support an en face orientation of a phenylalanine side chain at position 449 in *Shaker*, whereas Y82 in wild-type KcsA has an edge-on orientation. This fact alone suggests that the outer entrance to the permeation pathway can be structurally diverse and hints at the possibility that this region of the channel may also be structurally dynamic. Some type of structural malleability may help explain the surprising fact that the introduction of overtly charged residues at position 449, either Glu or Lys, greatly enhances the rate of slow inactivation, despite the large-magnitude electrostatic potentials that they carry. Our model would predict just the opposite effect. We are therefore forced to conclude that the charged side chains at this site produce other local changes in structure that dominate the gating kinetics by reducing the energy barrier for entry into the inactivated state.

Another possibility that we have not considered in detail is that the T449F mutation may completely abolish C-type inactivation, revealing a slower "U-type" inactivation, previously reported as a contributor to the slow inactivation in wild-type *Shaker* channels (Klemic et al., 2001). Although this mechanism is poorly understood in *Shaker*, one of its properties is that TEA does not manifest a foot-in-the-door inhibition in this type of inactivation. If indeed the T449F mutation unearths a slow U-type inactivation, our data suggest that these introduced aromatic side chains have an en face orientation, and that the observed inactivation is accompanied by a constriction of the external mouth of the channel. This possibility warrants further study.

Our results can be accounted for by a model in which the V438A mutation results in conformational changes in the vicinity of the selectivity filter that include the reorientation of the T449F aromatic from en face to edge-on, in a manner roughly opposite to the effect of the E71A alanine substitution in KcsA. Although the actual structural consequences of the V438A mutation in *Shaker* remain hypothetical, the functional data unambiguously show that residues at *Shaker* positions 438 and 449 play essential roles in stabilizing the selectivity filter and controlling slow inactivation. Future structures, combined with functional assays, will certainly elucidate these roles.

REFERENCES

Ader, C., R. Schneider, S. Hornig, P. Velisetty, E.M. Wilson, A. Lange, K. Giller, I. Ohmert, M.F. Martin-Eauclaire, D. Trauner, et al. 2008. A structural link between inactivation and block of a K+ channel. *Nat. Struct. Mol. Biol.* 15:605–612. doi:10.1038/nsmb.1430

Ahern, C.A., A.L. Eastwood, H.A. Lester, D.A. Dougherty, and R. Horn. 2006. A cation–π interaction between extracellular TEA and an aromatic residue in potassium channels. *J. Gen. Physiol.* 128:649–657. doi:10.1085/jgp.200609654

Baukrowitz, T., and G. Yellen. 1995. Modulation of K+ current by frequency and external [K+]: a tale of two inactivation mechanisms. *Neuron.* 15:951–960. doi:10.1016/0896-6273(95)90185-X

Bernèche, S., and B. Roux. 2005. A gate in the selectivity filter of potassium channels. *Structure.* 13:591–600. doi:10.1016/j.str.2004.12.019

Chakrapani, S., J.F. Cordero-Morales, and E. Perozo. 2007a. A quantitative description of KcsA gating I: macroscopic currents. *J. Gen. Physiol.* 130:465–478. doi:10.1085/jgp.200709843

Chakrapani, S., J.F. Cordero-Morales, and E. Perozo. 2007b. A quantitative description of KcsA gating II: single-channel currents. *J. Gen. Physiol.* 130:479–496. doi:10.1085/jgp.200709844

Choi, K.L., R.W. Aldrich, and G. Yellen. 1991. Tetraethylammonium blockade distinguishes two inactivation mechanisms in voltage-activated K+ channels. *Proc. Natl. Acad. Sci. USA.* 88:5092–5095. doi:10.1073/pnas.88.12.5092

Cordero-Morales, J.F., L.G. Cuello, and E. Perozo. 2006a. Voltage-dependent gating at the KcsA selectivity filter. *Nat. Struct. Mol. Biol.* 13:319–322. doi:10.1038/nsmb1070

Cordero-Morales, J.F., L.G. Cuello, Y. Zhao, V. Jogini, D.M. Cortes, B. Roux, and E. Perozo. 2006b. Molecular determinants of gating at the potassium-channel selectivity filter. *Nat. Struct. Mol. Biol.* 13:311–318. doi:10.1038/nsmb1069

Cordero-Morales, J.F., V. Jogini, A. Lewis, V. Vásquez, D.M. Cortes, B. Roux, and E. Perozo. 2007. Molecular driving forces determining potassium channel slow inactivation. *Nat. Struct. Mol. Biol.* 14:1062–1069. doi:10.1038/nsmb1309

Doyle, D.A., J. Morais Cabral, R.A. Pfuetzner, A.L. Kuo, J.M. Gulbis, S.L. Cohen, B.T. Chait, and R. MacKinnon. 1998. The structure of the potassium channel: molecular basis of K+ conduction and selectivity. *Science.* 280:69–77. doi:10.1126/science.280.5360.69

Foster, J.M., and S.F. Boys. 1960. Canonical configurational interaction procedure. *Rev. Mod. Phys.* 32:300–302. doi:10.1103/RevModPhys.32.300

Goldstein, S.A.N., and C. Miller. 1993. Mechanism of charybdotoxin block of a voltage-gated K+ channel. *Biophys. J.* 65:1613–1619. doi:10.1016/S0006-3495(93)81200-1

Grissmer, S., and M. Cahalan. 1989. TEA prevents inactivation while blocking open K+ channels in human T lymphocytes. *Biophys. J.* 55:203–206. doi:10.1016/S0006-3495(89)82793-6

Heginbotham, L., M. LeMasurier, L. Kolmakova-Partensky, and C. Miller. 1999. Single *streptomyces lividans* K+ channels: functional asymmetries and sidedness of proton activation. *J. Gen. Physiol.* 114:551–560. doi:10.1085/jgp.114.4.551

Hoshi, T., W.N. Zagotta, and R.W. Aldrich. 1991. Two types of inactivation in Shaker K+ channels: effects of alterations in the carboxy-terminal region. *Neuron.* 7:547–556. doi:10.1016/0896-6273(91)90367-9

Kavanaugh, M.P., M.D. Varnum, P.B. Osborne, M.J. Christie, A.E. Busch, J.P. Adelman, and R.A. North. 1991. Interaction between tetraethylammonium and amino acid residues in the pore of cloned voltage-dependent potassium channels. *J. Biol. Chem.* 266:7583–7587.

Kiss, L., J. LoTurco, and S.J. Korn. 1999. Contribution of the selectivity filter to inactivation in potassium channels. *Biophys. J.* 76:253–263. doi:10.1016/S0006-3495(99)77194-8

Klemic, K.G., G.E. Kirsch, and S.W. Jones. 2001. U-type inactivation of Kv3.1 and *Shaker* potassium channels. *Biophys. J.* 81:814–826. doi:10.1016/S0006-3495(01)75743-8

Lenaeus, M.J., M. Vamvouka, P.J. Focia, and A. Gross. 2005. Structural basis of TEA blockade in a model potassium channel. *Nat. Struct. Mol. Biol.* 12:454–459. doi:10.1038/nsmb929

Liu, Y., M.E. Jurman, and G. Yellen. 1996. Dynamic rearrangement of the outer mouth of a K+ channel during gating. *Neuron.* 16:859–867. doi:10.1016/S0896-6273(00)80106-3

López-Barneo, J., T. Hoshi, S.H. Heinemann, and R.W. Aldrich. 1993. Effects of external cations and mutations in the pore region on C-type inactivation of Shaker potassium channels. *Receptors Channels.* 1:61–71.

Ma, J.C., and D.A. Dougherty. 1997. The Cationminus signpi Interaction. *Chem. Rev.* 97:1303–1324. doi:10.1021/cr9603744

MacKinnon, R., and G. Yellen. 1990. Mutations affecting TEA blockade and ion permeation in voltage-activated K+ channels. *Science.* 250:276–279. doi:10.1126/science.2218530

Molina, A., A.G. Castellano, and J. López-Barneo. 1997. Pore mutations in *Shaker* K+ channels distinguish between the sites of tetraethylammonium blockade and C-type inactivation. *J. Physiol.* 499:361–367.

Murphy, R.B., M.D. Beachy, R.A. Friesner, and M.N. Ringnalda. 1995. Pseudospectral localized Møller-Plesset methods: theory and calculation of conformational energies. *J. Chem. Phys.* 103:1481–1490. doi:10.1063/1.469769

Nowak, M.W., P.C. Kearney, J.R. Sampson, M.E. Saks, C.G. Labarca, S.K. Silverman, W. Zhong, J. Thorson, J.N. Abelson, N. Davidson, et al. 1995. Nicotinic receptor binding site probed with unnatural amino acid incorporation in intact cells. *Science.* 268:439–442. doi:10.1126/science.7716551

Nowak, M.W., J.P. Gallivan, S.K. Silverman, C.G. Labarca, D.A. Dougherty, and H.A. Lester. 1998. In vivo incorporation of unnatural amino acids into ion channels in Xenopus oocyte expression system. *Methods Enzymol.* 293:504–529. doi:10.1016/S0076-6879(98)93031-2

Saebo, S., and P. Pulay. 1993. Local treatment of electron correlation. *Annu. Rev. Phys. Chem.* 44:213–236. doi:10.1146/annurev.pc.44.100193.001241

Santarelli, V.P., A.L. Eastwood, D.A. Dougherty, C.A. Ahern, and R. Horn. 2007. Calcium block of single sodium channels: role of a pore-lining aromatic residue. *Biophys. J.* 93:2341–2349. doi:10.1529/biophysj.107.106856

Stansfeld, P.J., A. Grottesi, Z.A. Sands, M.S. Sansom, P. Gedeck, M. Gosling, B. Cox, P.R. Stanfield, J.S. Mitcheson, and M.J. Sutcliffe. 2008. Insight into the mechanism of inactivation and pH sensitivity in potassium channels from molecular dynamics simulations. *Biochemistry.* 47:7414–7422. doi:10.1021/bi800475j

Starkus, J.G., L. Kuschel, M.D. Rayner, and S.H. Heinemann. 1997. Ion conduction through C-type inactivated *Shaker* channels. *J. Gen. Physiol.* 110:539–550. doi:10.1085/jgp.110.5.539

Yeh, J.Z., and C.M. Armstrong. 1978. Immobilisation of gating charge by a substance that simulates inactivation. *Nature.* 273:387–389. doi:10.1038/273387a0

Yellen, G. 1998. The moving parts of voltage-gated ion channels. *Q. Rev. Biophys.* 31:239–295. doi:10.1017/S0033583598003448

Yellen, G. 2002. The voltage-gated potassium channels and their relatives. *Nature.* 419:35–42. doi:10.1038/nature00978

Yellen, G., D. Sodickson, T.-Y. Chen, and M.E. Jurman. 1994. An engineered cysteine in the external mouth of a K+ channel allows inactivation to be modulated by metal binding. *Biophys. J.* 66:1068–1075. doi:10.1016/S0006-3495(94)80888-4